African Journal of Applied Research
Vol. 12, No. 4 (2026), pp.350-376
http://www.ajaronline.com
https://doi.org/10.26437
Received November22, 2025
Peer reviewed: April 15, 2026
Revised: May 15, 2026
Published: June 30, 2026

A HYBRID MOBILENETV2–SNAKE OPTIMISER FRAMEWORK FOR AUTOMATED RETINAL DISEASE RECOGNITION USING FUNDUS PHOTOGRAPHY

Chaid, A. M.[1], Sadoon, R. N.[2], Ali, Z. H.[3], Mahmood, S. S.[4], and Haitham Abdul Amir, A.[5]

[1] *Department of Computer Science, College of Computer Science and Information Technology, University of Basra, Basra, Iraq.*
[2&4] *College of Administration and Economics, University of Basrah, Iraq.*
[3] *Department of Geology, College of Science, University of Basra, Basra, Iraq.*
[5] *Department of Computer Science, Shatt Al-Arab University College, Basra, Iraq.*
[1]*adala.gyad@uobasrah.edu.iq*
[2]*ruaa.nabeel@uobasrah.edu.iq*
[3]*zahraa.ali@uobasrah.edu.iq*

ABSTRACT

Purpose: This study aims to develop an intelligent framework that automatically identifies major retinal diseases from fundus images and improves diagnostic performance by optimising deep learning hyperparameters.

Design/Methodology/Approach: A deep learning framework was developed using transfer learning and evaluated on retinal fundus images across four categories: cataract, glaucoma, diabetic retinopathy, and normal. Three pretrained convolutional neural network architectures, namely MobileNetV2, VGG16, and InceptionV3, were investigated and compared. Image preprocessing procedures were applied before training, including resizing, normalisation, and label encoding. To further enhance performance, the Snake Optimiser was employed to search for the most suitable hyperparameter settings of the best-performing network. Model effectiveness was assessed using accuracy, precision, recall, and F1-score.

Research Limitation: The proposed framework was validated using a single retinal image dataset containing four disease categories. The study did not include external clinical validation or multimodal ophthalmic data, which may further improve generalizability and diagnostic reliability in real-world healthcare environments.

Findings: The comparative analysis showed that MobileNetV2 achieved superior performance among the evaluated architectures before optimisation. After integrating the Snake Optimiser, the classification performance improved substantially, reaching an overall accuracy of 96.33%. The optimised model demonstrated excellent capability in distinguishing retinal disease

ISSN: 2408-7920

African Journal of Applied Research
Vol. 12, No. 4 (2026), pp.350-376
http://www.ajaronline.com
https://doi.org/10.26437
Received November22, 2025
Peer reviewed: April 15, 2026
Revised: May 15, 2026
Published: June 30, 2026
categories, achieving particularly high performance in cataract detection with precision, recall, and F1-score values approaching perfect classification.
Practical Implication: The developed framework offers a reliable decision-support mechanism for ophthalmic screening programs. Its ability to deliver accurate predictions with relatively low computational requirements makes it suitable for implementation in resource-constrained healthcare facilities.
Social Implication: Early identification of retinal abnormalities can facilitate timely treatment and reduce the risk of avoidable blindness. The proposed approach may support broader access to eye disease screening services, especially in regions where specialised ophthalmic expertise is scarce.
Originality/Value: The novelty of this work lies in combining a lightweight transfer learning architecture with a bio-inspired optimisation algorithm to enhance retinal disease classification. The integration of MobileNetV2 and Snake Optimiser provides an effective strategy for improving diagnostic accuracy while maintaining computational efficiency, offering a valuable contribution to computer-aided ophthalmic diagnosis.

Keywords: *Deep learning. fundus imaging. mobilenetv2. retinal disease. Snake Optimiser. transfer learning*

INTRODUCTION

The retina is the light-sensitive layer lining the inner rear of the eye. Its essential function is to convert incoming light into neural signals. These signals are transmitted to the brain's visual cortex for processing and object recognition (Ayzenberg et al., 2022).The retina may sustain irreparable damage from undiagnosed eye conditions, resulting in irreversible visual loss. Consequently, early detection is essential for timely and appropriate treatment (Bourne et al., 2013; Congdon et al., 2004). As such, various imaging methods for the retina have been developed to diagnose eye diseases. Among these techniques, Colour Fundus Photography (CFP) and Optical Coherence Tomography (OCT) are the most common (Li et al., 2021).

OCT imaging helps capture high-resolution cross-sectional images. This can help measure the retinal thickness and facilitate the effective diagnosis of eye diseases. The main challenge of this technique is its high costs. On the contrary, CFP generates fundus pictures that help visualise the internal surfaces of an eye. It is a cheap, non-invasive, and practical procedure for detecting retinal diseases. To promote the early diagnosis of eye disease, people are often encouraged to receive routine eye examinations using CFP, especially adults (Li et al., 2020). Fundus images acquired via CFP are used by ophthalmologists to effectively diagnose a myriad

ISSN: 2408-7920

African Journal of Applied Research
Vol. 12, No. 4 (2026), pp.350-376
http://www.ajaronline.com
https://doi.org/10.26437
Received November22, 2025
Peer reviewed: April 15, 2026
Revised: May 15, 2026
Published: June 30, 2026

of conditions, such as cataracts, diabetic retinopathy, glaucoma, and other retinal diseases (Orfao & van der Haar, 2021).

Causes of cataracts include ageing, genetic disposition, trauma, abnormalities of the immune system, metabolic disorders, and exposure to radiation. Ageing and oxidative damage result in the deposition of denatured protein, leading to the opacity of the lens and, ultimately, inhibiting light from reaching the retina (Keenan et al., 2022).

One of diabetes's consequences, diabetic retinopathy, is brought on by persistently high blood glucose levels. This disease causes damage to the blood vessels within the retina, resulting in leaking of fluid and blood that can eventually lead to complete sight loss if not treated (Farooq et al., 2022). Glaucoma is an irreversible and progressive condition, which is characterised by optic disc atrophy, visual field defects, and progressive visual impairment. The second is known to be associated with high intraocular pressure and low optic nerve blood flow (Prananda et al., 2022).

One of the main problems with eye diseases is that the initial symptoms are similar across diseases, making early diagnosis difficult. Furthermore, generating such a large number of images with CFP makes manual analysis time-consuming and labour-intensive. In developing countries such as India, where the number of ophthalmologists is very low, the situation is worse. As a result, creating automated diagnostic systems has gained paramount attention for improving diagnostic accuracy, minimising specialists' workload, and providing effective decision support.

CNNs belong to a family of computer-aided diagnostic tools and have demonstrated the ability to analyse biomedical images, including retinal images. CNNs have achieved excellent performance on the classification of eye diseases. They offer numerous benefits, such as reduced diagnosis time and a minimised burden on doctors. In this way, CNN-based systems can help achieve early diagnosis and, in turn, facilitate interventions that can mitigate more severe problems, such as blindness.

LITERATURE REVIEW

In this section, we discuss some of the works that have been performed in eye disease diagnosis. For instance, Junjun et al. (2021)have introduced a new network, DCNet, for multi-marker classification of eye ailments. This DCNet comprises 3 primary components: a spatial correlation unit to correlate features, a backbone to extract features from fundus images, and a

African Journal of Applied Research
Vol. 12, No. 4 (2026), pp.350-376
http://www.ajaronline.com
https://doi.org/10.26437
Received November22, 2025
Peer reviewed: April 15, 2026
Revised: May 15, 2026
Published: June 30, 2026

categorisation unit. On the other hand, Gour and Khanna (2021) have introduced four CNN architectures optimised using diverse algorithms. Using the Ocular Disease Intelligent Recognition (ODIR) dataset, these architectures are then deployed to classify multi-class fundus images. This ODIR dataset shows alterations of important anatomical features, including the macula, blood vessels, and the optic disc. The results showed that, among the 4 architectures, VGG16 paired with the SGD optimiser outperformed the others in classifying fundus images.

To enhance fundus image analysis for disease diagnosis, Luo et al. (2021) developed a deep learner that integrates an assortment of loss functions. By integrating focused loss robustness into the loss function, the model improved its classification performance on eye disease datasets. To facilitate retinal vasculature segmentation from CFP images, Hu et al. (2018) have developed a CNN-based methodology. The approach generates probability maps using CNN and loss functions, using feature maps to precisely extract retinal vascular information.

Based on the convolutional architecture reinforced with supervised learning, Playout et al. (2019) have presented a technique that is trained on the Messidor dataset. At the pixel level, this technique detects and confirms red and brilliant lesions. The results indicate this method achieves an Area Under Curve (AUC) score of 83.9%. To facilitate cataract detection from fundus images, (Pahuja et al., 2022) have introduced a hybrid model using CNN and Support Vector Machine (SVM). After augmenting the dataset and extracting features, the CNN achieved 87.08% accuracy, while the SVM achieved 87.5% accuracy.

Based on loss function optimisation techniques to reduce complexity, Junayed et al. (2021) developed the CataractNet model for cataract detection. The results indicate that this model is efficient and requires few parameters and kernels. On the other hand, a deep learning model for cataract diagnosis is presented in Tham et al. (2022) and is trained on CFP images. The outcome indicated that an AUC of 96.6% was attained, significantly higher than the four ophthalmologists' average of 91.6%. Based on Faster CNN and Hough Transform, (Jiang et al., 2021) have presented approaches to enhance cataract detection. Grad-CAM and t-SNE were used to refine lens opacity scores and focus on regions of interest.

To provide efficient cataract classification, Elloumi (2021) introduced a MobileNet-V2 model. This method combines random forest algorithm, and feature extraction with MobileNet-V2 for cataract severity prediction. This approach achieved 90.68% and 91.43% accuracy and sensitivity, respectively. Based on augmented fundus images, Ryu et al. (2021) developed a DenseNet-169 model for the detection and classification of retinopathy severity. The results

ISSN: 2408-7920

African Journal of Applied Research
Vol. 12, No. 4 (2026), pp.350-376
http://www.ajaronline.com
https://doi.org/10.26437
Received November22, 2025
Peer reviewed: April 15, 2026
Revised: May 15, 2026
Published: June 30, 2026

indicate that this model attained an accuracy of 90%. On the other hand, Mushtaq and Siddiqui (2021) present a fully automated CNN-based model for predicting diabetic retinopathy (DR). Using fluorescein angiography, the model achieved 91% accuracy and 86% sensitivity.

To determine whether fundus images are either healthy or indicative of retinopathy, a hybrid inductive machine learning method (HIMLM) is introduced by Mahmoud et al. (2023). After normalising the picture brightness, the developed model performs feature extraction, segmentation, and classification using the encoder-decoder approach. The results indicate that the model attains accuracy and sensitivity of 96.62% and 95.31%, respectively. To diagnose glaucoma, a CNN framework is presented by (Veena et al., 2022). This framework segments the optic disc and optic cup while computing the cup-to-disc ratio. The outcome indicated that an optic cup segmentation accuracy of 97% was attained, while optic disc segmentation accuracy was 98%.

On the other hand, a two-branch convolutional network is developed by Abdel-Hamid (2022) for the extraction of anatomical features of optic discs and blood vessels. The comparison of subbands was combined with the retina's spatial input to yield a wavelet approximation for computation. The results obtained indicated 96.34% accuracy for wavelet inputs and 98.78% accuracy for spatial inputs. To refine the disc boundaries and enhance the cup-to-disc ratio, a deep learning network is introduced by Chang et al. (2021), based on fundus images. The outcome indicated an improvement in glaucoma diagnosis, with interpretations based on Grad-CAM and adversarial examples.

A deep learning network was trained on fundus images to refine disc boundaries and enhance the cup-to-disc ratio, thereby improving glaucoma diagnosis from these images. The results were interpreted using adversarial examples and Grad-CAM (Chang et al., 2021). To differentiate between eye colours for detecting glaucoma, a combined approach is introduced (Nawaz et al., 2022).

In this technique, EfficientNet-B0 is used to differentiate lesions, while EfficientDet-D0 is used to differentiate eye colour. Here, features are extracted with EfficientNet-B0 and processed with EfficientDetD0. On the other hand, Thanki (2023) proposed CNN along with a machine learning-based intelligent hybrid system, which performs analysis of fundus images for glaucoma diagnosis. In this system, feature extraction is accomplished using CNN, while machine learning techniques are utilised for classification. The results indicate that logistic regression yields the best outcomes. Using Gaussian kernels and entropy-based thresholding to preserve blood vessels, three CNN models are developed by Kumar and Singh (2023) for

African Journal of Applied Research
Vol. 12, No. 4 (2026), pp.350-376
http://www.ajaronline.com
https://doi.org/10.26437
Received November22, 2025
Peer reviewed: April 15, 2026
Revised: May 15, 2026
Published: June 30, 2026

predicting retinal diseases. On the other hand, Thanki (2022) has deployed multiple classifiers (CNN, RF, SVM, DT) for detecting retinal disease, with CNN showing the best performance. Table 1 presents a comparison of these related works.

Table 1: Comparison of eye disease diagnosis techniques

Reference	Proposed Method	Description	Dataset/Technique	Performance
(Junjun et al., 2021)	DCNet	Three-unit network: feature extraction, spatial correlation, and Classification	Fundus images	–
(Gour & Khanna, 2021)	CNN models that have optimizers	VGG16 with SGD optimiser for fundus image classification	ODIR dataset	VGG16 with SGD outperformed others
(Luo et al., 2021)	Using mix loss in deep learning	Combines mixture loss and focal loss robustness for better classification	Eye disease datasets	Improved classification
(Hu et al., 2018)	Retinal vasculature segmentation	CNN model with loss function and feature maps for detailed segmentation	CFP images	Precise segm entation
(Playout et al., 2019)	Messidor dataset analysis	System for red and bright lesion segmentation	Messidor dataset	AUC: 83.9%
(Pahuja et al., 2022)	SVM+ CNN	Hybrid approach for cataract detection using augmented images	Fundus images	CNN: 87.08%, SVM: 87.5%
(Junayed et al., 2021)	CataractNet	Optimized loss function for computational efficiency	Fundus images	–

ISSN: 2408-7920

African Journal of Applied Research
Vol. 12, No. 4 (2026), pp.350-376
http://www.ajaronline.com
https://doi.org/10.26437
Received November22, 2025
Peer reviewed: April 15, 2026
Revised: May 15, 2026
Published: June 30, 2026

(Tham et al., 2022)	Using deep learning to identify cataracts	High AUC compared to oph-thalmologists' performance	CFP images	AUC: 96.6%
(Jiang et al., 2021)	Grad-CAM for the identification of cataracts	Combines Hough Transform and Faster CNN for enhanced accuracy	Fundus images	–
(Elloumi, 2021)	MobileNet-V2 with random forest	Lightweight model for cataract classification	Fundus images	Accuracy: 90.68%, Sensitivity: 91.43%
(Ryu et al., 2021)]	DenseNet-169	Retinopathy detection with image augmentation	Fundus images	Accuracy: 90%
(Mushtaq & Siddiqui, 2021)	Completely automatic categorizati on of DRs	CNN with fluorescein angiography	Fluorescein angiography	Accuracy: 91%, Sensitivity: 86%
(Mahmoud et al., 2023)	Machine learning that is hybrid inductive (HIMLM)	Brightness normalization, encodingdecoding, segmentation, feature extraction	Fundus images	Accuracy: 96.62%, Sensitivity: 95.31%
(Veena et al., 2022)	Optic cup and disc segmentation	The cup-to-disc ratio is used to diagnose glaucoma	Fundus images	Optic cup: 97%, Optic disc: 98%
(Abdel-Hamid, 2022)	CNN with two branches	Eextracts blood vessel and optic disc anatomical Characteristics	Subband comparison and wavelet approximation	Accuracy: 98.78% (spatial), 96.34% (wavelet)
(Chang et al., 2021)	Deep learning with Grad-CAM	Detecting glaucoma	Fundus images	–

ISSN: 2408-7920

African Journal of Applied Research
Vol. 12, No. 4 (2026), pp.350-376
http://www.ajaronline.com
https://doi.org/10.26437
Received November22, 2025
Peer reviewed: April 15, 2026
Revised: May 15, 2026
Published: June 30, 2026

		with adversarial instances and cup-to-disc ratio refinement		
(Nawaz et al., 2022)	EffectiveNet-B0 and EffectiveDetD0	Features extracted and combined using BiFPN module	Fundus images	–
(Thanki, 2023)	Hybrid CNN and ML	Feature extraction with CNN, classification with ML algorithms	Fundus images	Logistic regression outperformed others
(Kumar & Singh, 2023)	Three types of CNN	Gaussian kernel optimisation and entropy-based blood vessel extraction	Fundus images	–
(Thanki, 2022)	RF, SVM, CNN and DT models	Comparative analysis for retinal disease classification	Retinal dataset	CNN outperformed others

METHODOLOGY

This paper develops a reliable retina disease detection and prediction system through fundus image classification. The first step is exploratory data analysis (EDA), in which the dataset is examined to assess its shape, class distribution, and potential issues, such as class imbalance or missing data. Afterwards, we preprocess the images so that they all have the same height and width dimensions and undergo pixel normalisation according to the requirements of deep learning models (DLMs).

The CNNs VGG16, MobileNetV2, and InceptionV3, as well as the DLM, are trained on the pre-processed data. We selected the following models, each with a unique architecture, to compare their performance. The ocular diseases to be classified included glaucoma, cataract, and diabetic retinopathy. Comparisons are then made against a normal eye. To improve performance, the models' architectures and hyperparameters were fine-tuned. To dynamically

ISSN: 2408-7920

African Journal of Applied Research
Vol. 12, No. 4 (2026), pp.350-376
http://www.ajaronline.com
https://doi.org/10.26437
Received November22, 2025
Peer reviewed: April 15, 2026
Revised: May 15, 2026
Published: June 30, 2026

fine-tune hyperparameters, a new optimisation method, the Snake Optimiser, is utilised. To achieve the highest possible model accuracy and efficiency, most favourable parameters (including the number of units in each dense layer, dropout rate, and learning rate) are chosen as part of the optimisation process.

After training, the models' performance is evaluated using measures such as precision, confusion matrix analysis, accuracy, F1-score, and recall. To determine the most suitable architecture for the classification task, performance is compared across these models. In addition, learning curves and confusion matrices, which reveal each model's advantages and disadvantages, allow us to visually assess each model's performance. The proposed methodology is illustrated in Figure 1. The following sub-sections discuss each approach of the methodology in detail. This includes the methods employed for EDA, preprocessing, model training, and evaluation.

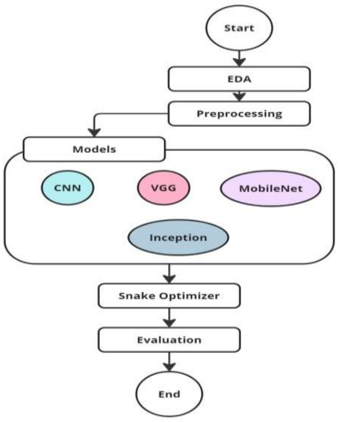

Figure 1: Workflow of the Proposed Methodology

Description of Dataset

This study utilised the "Eye Diseases Classification" dataset, which was unnamed until investigation. It contained retinal photographs that were categorised into four distinct groups. Normal ones, those caused by diabetic retinopathy, cataracts, and glaucoma are all available. Each category has around 1,000 photos. Testing and training are complementary processes. Pictures come from a variety of sources, including HRF, Ocular Recognition, and IDRiD, to ensure the collection is strong and varied. Figure 2 shows an example of a retinal picture from each group. Rows one through three include normal, cataract, and glaucoma. In the second row, we can see eye disorders such as cataracts, diabetic retinopathy, and glaucoma. Deep

ISSN: 2408-7920

African Journal of Applied Research
Vol. 12, No. 4 (2026), pp.350-376
http://www.ajaronline.com
https://doi.org/10.26437
Received November22, 2025
Peer reviewed: April 15, 2026
Revised: May 15, 2026
Published: June 30, 2026

learning algorithms rely on these images to properly identify and classify diseases because they show the unique symptoms of each condition.

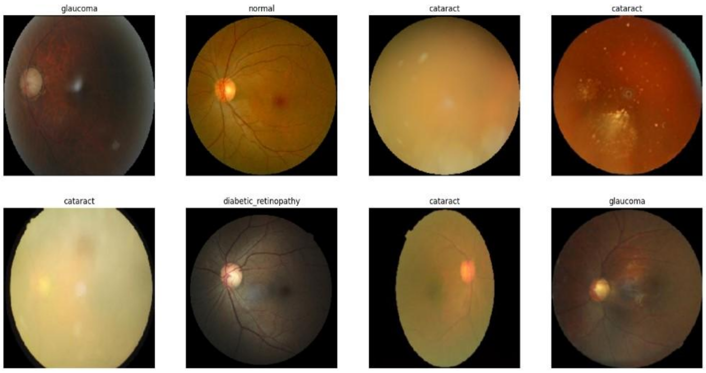

Figure 2: Example images of the retina from the dataset, as grouped by class (Glaucoma, Normal, Cataract, and Diabetic Retinopathy)

Exploratory Data Analysis and Preprocessing

The exploratory data analysis (EDA) method included examining the dataset's structure and class distribution. The dataset has four classes: Cataract, Diabetic Retinopathy, Glaucoma, and Normal, representing various retinal images. There are around 1,000 images in each class, which gives us a balanced dataset. The number of images per class was also checked as a measure of balance during EDA, and sample images from each class were reviewed to assess visual variation.

The ultimate objective of the first stage is to preprocess the data for training a deep learning model. In accordance with traditional convolutional neural network architectures, all photos were first scaled to match the target resolution of 224 × 224 pixels. Images were subsequently normalised to the range [0,1], which helps accelerate model convergence during training. The labels were encoded to the corresponding integers for each class, then one-hot encoded to enable the data to support multi-class classification tasks.

To measure model performance, the developed model was trained and validated using an 80%/20 % split, despite the dataset's dual nature. Stratified sampling was used to maintain the class distribution in both sets. Once the models had been trained on the training sets, the remaining verification sets were used to validate them. Such preprocessing was essential for

ISSN: 2408-7920

African Journal of Applied Research
Vol. 12, No. 4 (2026), pp.350-376
http://www.ajaronline.com
https://doi.org/10.26437
Received November22, 2025
Peer reviewed: April 15, 2026
Revised: May 15, 2026
Published: June 30, 2026

preparing the data for deep learning while also avoiding common issues such as overfitting or underfitting.

Transfer Learning Models

In this experiment, the basic architecture of the transfer learning model focused on the retinal disease classification task. The first model is a custom CNN defined as follows: the input layer accepts images with dimensions 224×224×3. Three convolutional blocks are then applied, where each block contains a convolutional and a max-pooling layer. Convolutional layers' activation function was the Rectified Linear Unit (ReLU), while the kernel size was set to 3 × 3.

In addition, filters of increasing sizes (that is, 64, 128, and 256) were deployed. To minimise execution complexity and spatial dimensions, we deployed max-pooling layers with a pool size of 2 × 2. After the feature extraction layers, the proposed model's flattening layer transformed 2D feature maps into 1D vectors. After that, there were output, dense, and dropout layers that were deployed for multi-class classification, activation, and regularisation, respectively. Here, the final output layer comprised a softmax activation and four units. On the other hand, the dense layer consisted of 256 units and a ReLU. On its part, the dropout layer had a rate of 0.2 for the said regularisation.

The VGG16 networks were loaded from ImageNet with weights on their pretrained VGG16 architecture. Next, we loaded the base model (without the top classification layer), froze its convolutional layers, and used it as a fixed feature extractor. To minimise feature dimensions, a global mean pooling layer is initially deployed to the features. Thereafter, custom layers are built on top of these base modules. Next are 128- and 256-unit dense layers with ReLU activation, followed by dropout layers with rates of 0.1 and 0.3. Here, softmax activation is used for categorisation in four of the units in our final output unit group.

The MobileNetV2 model is based on a pretrained MobileNetV2 architecture and is also initialised from an ImageNet-pretrained model (without the final classification layer). This facilitates the preservation of the features learned during the pretraining, as the base layers are frozen. From there, additional custom layers are added, beginning with a global mean-pooling layer that acts as a feature deconsolidator, and gradually feeding dense layers of 1024, 512, 256, and 128 with ReLU activations. To classify the retinal disease classes, a 0.2 rate dropout layer is applied. The final output layer consists of a softmax activation function and four units.

African Journal of Applied Research
Vol. 12, No. 4 (2026), pp.350-376
http://www.ajaronline.com
https://doi.org/10.26437
Received November22, 2025
Peer reviewed: April 15, 2026
Revised: May 15, 2026
Published: June 30, 2026

The InceptionV3 model initialises the pretrained InceptionV3 architecture using ImageNet weights, but excludes the top classification layer. This freezes the base model weights, and therefore they are not updated. This is followed by a ReLU activation and a 1024-unit dense layer. Next is the global average pooling layer and a 0.3 rate dropout layer. In addition, there is a thick layer comprising 512 units and ReLU as the activation function.

In order to have half as many neurons in this layer as in the previous one (same input size), we also add a second 0.5 rate dropout layer. To classify retinal images, we include four units with a softmax activation at the output dense layer. In the proposed approach, the transfer learning networks use pretrained architectures to compute relevant features, while custom layers are designed for the specific problem of retinal disease classification. We determined the most suitable architecture for this task by training and evaluating each model on the same dataset. Table 2 presents some of the model settings and relevant parameters.

Table 1: Parameters and values for each model

Model	Parameter	Value
CNN	Input Shape Number of Concolutional Blocks Filter Sizes (per block) Kernel Sizes Pool Size Dense Layer Units Dropout Rate Output Layer Units	224 × 224 × 3 3 64, 128, 256 3 × 3 2 × 2 256 032 4 (Softmax activation)
VGG16	Pretrained Base	VGG16 (ImageNet weights)
	Input Shape	224 × 224 × 3
	Global Average Pooling Layer	Yes
	Dense Layer Units	256, 128
	Dropout Rates	0.1, 0.3
	Output Layer Units	4 (Softmax activation)
	Trainable Layers	Custom layers only
MobileNetV2	Pretrained Base	MobileNetV2 (ImageNet weights)
	Input Shape	224 × 224 × 3
	Global Average Pooling Layer	Yes

ISSN: 2408-7920

African Journal of Applied Research
Vol. 12, No. 4 (2026), pp.350-376
http://www.ajaronline.com
https://doi.org/10.26437
Received November22, 2025
Peer reviewed: April 15, 2026
Revised: May 15, 2026
Published: June 30, 2026

	Dense Layer Units	1024, 512, 256, 128
	Dropout Rate	0.2
	Output Layer Units	4 (Softmax activation)
	Trainable Layers	Custom layers only
InceptionV3	Pretrained Base	InceptionV3 (ImageNet weights)
	Input Shape	224 × 224 × 3
	Global Average Pooling Layer	Yes
	Dense Layer Units	1024, 512
	Dropout Rates	0.3, 0.5
	Output Layer Units	4 (Softmax activation)
	Trainable Layers	Custom layers only

Snake Optimiser

The Snake Optimiser (SO) is a new bio-inspired optimisation algorithm that efficiently adjusts hyperparameters for deep learning model training. This algorithm's modus operandi is similar to snakes when they find food: they have an exploration phase, which is followed by the exploitation phase. The procedure for the Snake Optimiser is depicted in Figure 3.

ISSN: 2408-7920

African Journal of Applied Research
Vol. 12, No. 4 (2026), pp.350-376
http://www.ajaronline.com
https://doi.org/10.26437
Received November22, 2025
Peer reviewed: April 15, 2026
Revised: May 15, 2026
Published: June 30, 2026

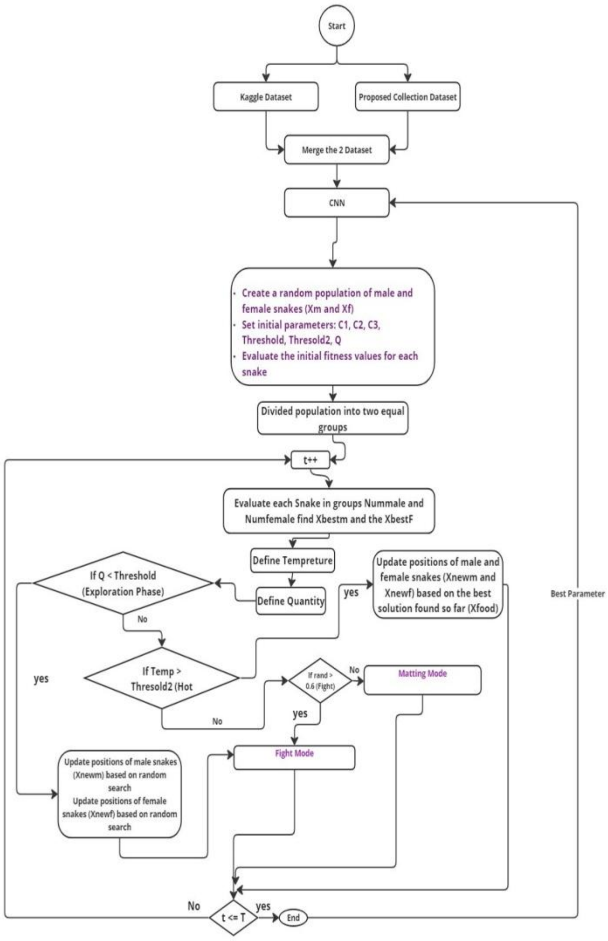

Figure 3: Workflow of the Snake Optimiser

The procedure begins with an initialisation step in which a uniform random population of snakes is created over predetermined boundaries. Each snake corresponds to a particular set of hyperparameters, such as dense layer units, dropout rates, learning rates, and batch sizes. We will calculate the snake's initial position using equation (1).

$$Xi = X\text{min} + r \cdot (X\text{max} - X\text{min}) \qquad (1)$$

ISSN: 2408-7920

African Journal of Applied Research
Vol. 12, No. 4 (2026), pp.350-376
http://www.ajaronline.com
https://doi.org/10.26437
Received November22, 2025
Peer reviewed: April 15, 2026
Revised: May 15, 2026
Published: June 30, 2026

Where Xi and r denote the location of the ith snake and a stochastic number in the range of 0 and 1. On the other hand, Xmin and Xmax represent lower and higher bounds of the search space, respectively. The population is then partitioned equally into female and male groups. Here, the number of males (Nm) and females (Nf) are determined by equation (2).

$$N_m = \frac{N}{2}, \quad N_f = N - N_m \tag{2}$$

Basically, each group evaluates its fitness based on the defined objective, and the best-performing male (Xbest, m) and female (Xbest, f) individuals are identified. Additionally, a "food source" (Xfood) is calculated as the global best solution found so far. The algorithm determines the food amount (Q) and temperature (T) using equation (3).

$$T = \exp\left(-\frac{t}{T_{\max}}\right), \quad Q = c_1 \cdot \exp\left(\frac{t - T_{\max}}{T_{\max}}\right) \tag{3}$$

where c1 is a constant, t is the iteration that is currently in progress, and Tmax is the highest number of iterations. In the exploration phase, provided that Q is below a predefined threshold ($Q < 0.25$), snakes perform random searches by updating their positions in accordance with equation (4).

$$Xi, m\,(t+1) = X\text{rand}, \text{m}(t) \pm c2 \cdot Am \cdot ((X\max - X\min) \cdot r + X\min \tag{4}$$

where Am is the ability of male snakes to locate food. A similar update rule applies to female snakes. In the exploitation phase, when $Q > 0.25$, the behaviour depends on the temperature. A high temperature ($T > 0.6$) causes snakes to head straight for the food source as in equation (5).

$$Xi, j\,(t+1) = X\text{food} \pm c3 \cdot T \cdot r \cdot (X\text{food} - Xi, j(t)) \tag{5}$$

If the temperature is low ($T \leq 0.6$), snakes switch to either Mating Mode (MM) or Fight Mode (FM). In FM, locations are updated in accordance with equation 6:

$$X_{i,\,m}\,(t+1) = X_{i,\,m}(t) + c_3 \cdot FM \cdot r \cdot (Q \cdot X_{\text{best, f}} - X_{i,\,m}(t) \tag{6}$$

In MM, male and female positions influence each other:

$$X_{i,\,m}\,(t+1) = X_{i,\,m}(t) + c_3 \cdot M_m \cdot r \cdot (Q \cdot X_{i,f}(t) - X_{i,\,m}(t)) \tag{7}$$

ISSN: 2408-7920

African Journal of Applied Research
Vol. 12, No. 4 (2026), pp.350-376
http://www.ajaronline.com
https://doi.org/10.26437
Received November22, 2025
Peer reviewed: April 15, 2026
Revised: May 15, 2026
Published: June 30, 2026

Throughout the optimisation, worst-performing snakes are replaced to maintain diversity. Solutions are iteratively improved by the method until convergence is achieved or the maximum number of iterations is reached.

This Snake Optimiser was performed to optimise the hyperparameters of the MobileNetV2 model, and the best hyperparameters identified were used for final training. The pseudocode of the Snake Optimiser and its workflow are depicted in Figure 3.

Algorithm 1: Snake Optimiser (SO)

Input: Population size N, maximum iterations $T_{\max}$, hyperparameter bounds [$X_{\min}$, $Xmax$], Thresholds {Threshold$_1$, Threshold$_2$}

Output: Best solution X_{best}

[1] Initialise random positions X_i for all snakes using:

$$X_i = X_{\min} + r \cdot (X_{\max} - X_{\min})$$

[2] Initialise velocities for all snakes and partition the population into two groups: Male (N_m) and Female

(N_f), where:

$$N_m = \frac{N}{2}, \quad N_f = N - N_m$$

[3] **For** iteration $t = 1$ to $T_{\max}$ **do**:

[4] Evaluate fitness of all snakes Identify {$X_{\text{best, m}}$}, {$X_{\text{best, f}}$}, and X_{food} (global best)

[5] Calculate T and Q as follows:

$$T = \exp\left(-\frac{t}{T_{\max}}\right), \quad Q = c_1 \cdot \exp\left(\frac{t - T_{\max}}{T_{\max}}\right)$$

[6] **If** $Q < Threshold_1$ **then**:

[7] Activate the ▷ exploration phase

[8] **For** each male snake $i \in N_m$ **do**:

Update position as follows:

$$X_{i,\,m}(t+1) = X_{\text{rand},\,m}(t) \pm c_2 \cdot A_m \cdot ((X_{\max} - X_{\min}) \cdot r + X_{\min})$$

[9] **end for**

[10] **For** each female snake $i \in N_f$ **do** :

[11] Update position as follows:

ISSN: 2408-7920

African Journal of Applied Research
Vol. 12, No. 4 (2026), pp.350-376
http://www.ajaronline.com
https://doi.org/10.26437
Received November22, 2025
Peer reviewed: April 15, 2026
Revised: May 15, 2026
Published: June 30, 2026

$$X_{i,f}(t+1) = X_{\text{rand},f}(t) \pm c_2 \cdot A_f \cdot ((X_{\text{max}} - X_{\text{min}}) \cdot r + X_{\text{min}})$$

[12] **end for**

[13] **else:**

[14] Activate ▷ exploitation phase

[15] **If** $T >$ Threshold$_2$ **then**:

[16] Activate ▷ hot phase

[17] **For** each snake *i* **do**:

[17] Move towards food as follows:

$$X_{i,j}(t+1) = X_{\text{food}} \pm c_3 \cdot T \cdot r \cdot (X_{\text{food}} - X_{i,j}(t))$$

[18] **end for**

[19] **else:**
[20] Activate ▷ cold phase
[21] Choose between *FM* or *MM* based on arbitrary probability

[22] **If** fight mode **then**:

[23] Update positions for males and females as follows:

$$X_{i,m}(t+1) = X_{i,m}(t) + c_3 \cdot FM \cdot r \cdot (Q \cdot X_{\text{best,f}} - X_{i,m}(t))$$

$$X_{i,f}(t+1) = X_{i,f}(t) + c_3 \cdot FF \cdot r \cdot (Q \cdot X_{\text{best,m}} - X_{i,f}(t))$$

[24] **else:**

[25] Activate ▷ mating mode

[26] Update positions as follows:

$$X_{i,m}(t+1) = X_{i,m}(t) + c_3 \cdot M_m \cdot r \cdot (Q \cdot X_{i,f}(t) - X_{i,m}(t))$$

ISSN: 2408-7920

African Journal of Applied Research
Vol. 12, No. 4 (2026), pp.350-376
http://www.ajaronline.com
https://doi.org/10.26437
Received November22, 2025
Peer reviewed: April 15, 2026
Revised: May 15, 2026
Published: June 30, 2026

$$X_{i,f}(t+1) = X_{i,f}(t) + c_3 \cdot M_f \cdot r \cdot (Q \cdot X_{i,m}(t) - X_{i,f}(t))$$

end if
end if
end if
Eliminate male and female snakes that are not performing well
end for
return X_{best} (best solution found)

RESULTS AND DISCUSSION

Results Before Optimisation

Before optimisation processes are implemented, performance metrics such as F1 score, accuracy, recall, and precision are used to assess model performance. MobileNetV2 was the model with the highest accuracy rating, at 89.81%. This shows that it works well at classifying retinal pictures. The proposed model achieved an F1 score of 89.88%, a recall of 89.81%, and an accuracy of 90.05%. The model's performance remains consistent across multiple tests, and all results are quite high.

MobileNetV2 achieves higher accuracy than VGG16, which is only 86.61% accurate. The model got an F1 score of 86.27%, with accuracy and recall rates of 86.67% and 86.61%, respectively. The findings show that VGG16 is a strong model for classification tasks; however, it is not as good as MobileNetV2. The third model tested, InceptionV3, got 83.41% correct. The F1-score is 83.38%, indicating recall of 83.41% and precision of 83.47%. With four times as many parameters, it works better than InceptionV3. But it can't beat MobileNetV2 and VGG16. The custom CNN model achieved the lowest accuracy, at 81.87%. The model's F1-score, recall, and precision were 81.93%, 81.87%, and 82.41%, respectively. The CNN didn't perform as well as the pretrained designs, but it achieved good accuracy. This shows that transfer learning works well for solving categorisation problems. Based on all the metrics before changing the model's hyperparameters, MobileNetV2 is clearly the best model. This shows that it can handle the difficulties of categorising retinal images.

ISSN: 2408-7920

African Journal of Applied Research
Vol. 12, No. 4 (2026), pp.350-376
http://www.ajaronline.com
https://doi.org/10.26437
Received November22, 2025
Peer reviewed: April 15, 2026
Revised: May 15, 2026
Published: June 30, 2026

Table 2: Performance prior to optimisation

Model	Accuracy (%)	Precision (%)	Recall (%)	F1-Score (%)
MobileNetV2	89.81	90.05	89.81	89.88
VGG16	86.61	86.67	86.61	86.27
InceptionV3	83.41	83.47	83.41	83.38
CNN	81.87	82.41	81.87	81.93

Results after Optimisation

The Snake Optimiser was used to improve MobileNetV2, as it was the most accurate among the initial models examined. By fine-tuning its hyperparameters, we were able to make a more efficient model. The Snake Optimiser raised the test accuracy to 96.33%, suggesting the data changed significantly. The optimisation strategy has significantly improved the model's efficacy in classifying retinal images. The model did a great job of finding and sorting photographs across all classes, achieving near-perfect F1-score, recall, and accuracy. The model achieved flawless recall and accuracy, resulting in a 99% F1 score for the Diabetic Retinopathy class. The model, on the other hand, was 96% accurate for glaucoma. The F1-score was 93%, while the recall was 91%. This class may have done well, but not great. The Normal class performed well, with an F1 Score of 94%, a recall of 97%, and an accuracy of 91%.

The findings demonstrate that the proposed model can assign Normal photos to the correct groups. But there are problems with accuracy. The overall class accuracy was 96.33%, with 96% for the weighted mean F1-score, precision, and recall, and 96% for the macro average recall, F1-score, and precision. These findings show that Snake Optimiser is a strong classifier for retinal illnesses, as it performed well with MobileNetV2. This finely calibrated model does a good job of predicting the likelihood of categorising distinct retinal events (i.e., it has high recall and accuracy).

Prediction Results

Using the optimised MobileNetV2 model, four categories were identified from retinal scans: Cataract, Diabetic Retinopathy, Glaucoma, and Normal. With each prediction, we attained good confidence scores, demonstrating the accuracy and reliability of the developed model. To visualise this performance, a bounding box is drawn over each input image, indicating the area the model considered when generating its prediction. The bounding box itself displays the predicted class label and corresponding confidence score.

ISSN: 2408-7920

African Journal of Applied Research
Vol. 12, No. 4 (2026), pp.350-376
http://www.ajaronline.com
https://doi.org/10.26437
Received November22, 2025
Peer reviewed: April 15, 2026
Revised: May 15, 2026
Published: June 30, 2026

The pictures below indicate what the model thinks will happen for each of the three classes. The full description of the categorisation and the model-derived confidence score for each figure are shown. This shows how well the model can find and categorise retinal problems. Figure 4 shows the expected retinal picture that was predicted to be a cataract.

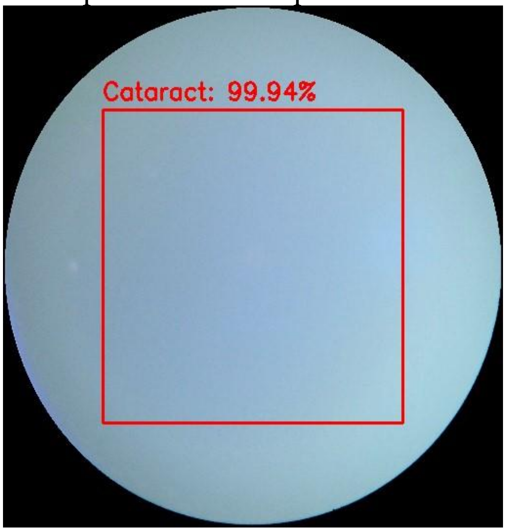

Figure 4: Cataract with confidence of 99.94% prediction

It could accurately forecast the condition with 99.94% accuracy, suggesting that it was very good at finding retinal symptoms of the disease. The bounding box shows where this categorisation is interested. Figure 5 shows how the model predicts diabetic retinopathy.

ISSN: 2408-7920

African Journal of Applied Research
Vol. 12, No. 4 (2026), pp.350-376
http://www.ajaronline.com
https://doi.org/10.26437
Received November22, 2025
Peer reviewed: April 15, 2026
Revised: May 15, 2026
Published: June 30, 2026

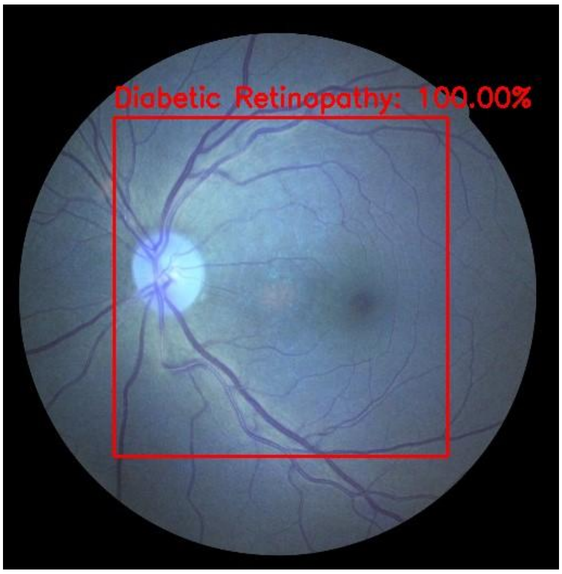

Figure 5: Diabetic Retinopathy Prediction with confidence of 100.00%.

The categorisation was successful with a confidence score of 100.00%. This shows that the model can find vascular problems that are signs of this ailment. Figure 6 shows how a retinal picture is classified as having glaucoma.

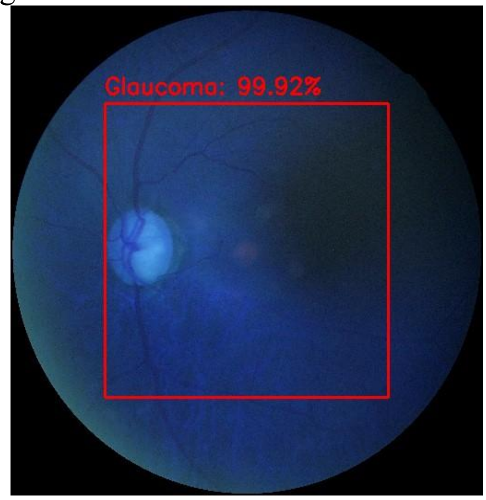

Figure 6: Prediction of Glaucoma with 99.92% confidence.

ISSN: 2408-7920

African Journal of Applied Research
Vol. 12, No. 4 (2026), pp.350-376
http://www.ajaronline.com
https://doi.org/10.26437
Received November22, 2025
Peer reviewed: April 15, 2026
Revised: May 15, 2026
Published: June 30, 2026

The model was 99.92% sure that this situation would happen. It does a good job of detecting signs of glaucoma, such as damage to the optic nerve. Figure 7 shows what the model thinks a normal retinal picture will look like.

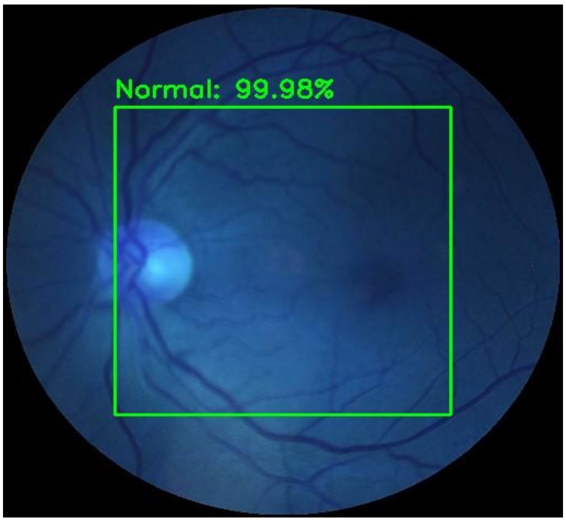

Figure 7: Prediction of Normal with 99.98% confidence

The classification was completed with 99.98% confidence. This shows how well the model can distinguish between healthy and diseased retinal images. Table 4 provides a comprehensive comparison of the proposed work with several other studies in the field of deep learning models for detecting retinal disorders.

ISSN: 2408-7920

African Journal of Applied Research
Vol. 12, No. 4 (2026), pp.350-376
http://www.ajaronline.com
https://doi.org/10.26437
Received November22, 2025
Peer reviewed: April 15, 2026
Revised: May 15, 2026
Published: June 30, 2026

Table 3: Comparisons with related works

Reference	Proposed Method	Dataset/technique	Performance
(Pahuja et al., 2022)	CNN + SVM	Fundus images with hybrid approach for cataract detection using augmented images	CNN: 87.08%, SVM: 87.5%
(Elloumi, 2021)	Random Forest using MobileNet-V2	Lightweight model for cataract classification using fundus images	Accuracy: 90.68%, Sensitivity: 91.43%
(Ryu et al., 2021)	DenseNet-169	Retinopathy detection with image augmentation using fundus images	Accuracy: 90%
(Mushtaq & Siddiqui, 2021)	CNN-based fully automatic DR classification	Fluorescein angiography dataset	Accuracy: 91%, Sensitivity: 86%
(Mahmoud et al., 2023)	Hybrid inductive machine learning (HIMLM)	Brightness normalisation, encoding-decoding, segmentation, feature extraction on fundus images	Accuracy: 96.62%, Sensitivity: 95.31%
Proposed Work	MobileNetV2 optimised with Snake Optimiser	Fundus images, hyperparameter tuning for improved retinal disease classification	Accuracy: 96.33%, Cataract Precision: 100%, Recall: 98%, F1-Score: 99%

Table 4 displays the methods employed, the datasets or procedures used, the accuracy, and other performance metrics collected. Pahuja et al. (2022) were able to diagnose cataracts with 87.08% accuracy for CNN and 87.5% for SVM using a hybrid method that combined both models. Elloumi (2021) did achieve a sensitivity of 91.43% and an accuracy of 90.68% when they used MobileNet-V2 with a random forest classifier. This shows that it works well for categorising lightweight cataracts. In the same way, Ryu et al. (2021) were able to find retinopathy 90% of the time using the DenseNet-169 model and image augmentation.

ISSN: 2408-7920

African Journal of Applied Research
Vol. 12, No. 4 (2026), pp.350-376
http://www.ajaronline.com
https://doi.org/10.26437
Received November22, 2025
Peer reviewed: April 15, 2026
Revised: May 15, 2026
Published: June 30, 2026

In the work of Mushtaq and Siddiqui, (2021) fully automated CNN-based classification system was applied to the diagnosis of diabetic retinopathy using fluorescein angiography. This system yields an accuracy of 91% and a sensitivity of 86%. On the other hand, Mahmoud et al. (2023) proposed a hybrid inductive machine learning method, achieving an accuracy of 96.62% and a sensitivity of 95.31% on fundus images.

The proposed model, which uses Snake Optimise together with MobileNetV2, outperformed previous approaches by a significant margin. It achieved high precision, recall, and F1 scores across several retinal disease types, with an accuracy of 96.33%. For example, the model achieved 100% precision, 98% recall, and 99% F1-score for cataract detection. This demonstrates that Snake Optimise successfully improved the MobileNetV2 model for precise and trustworthy categorisation of retinal diseases.

CONCLUSION

This work demonstrated how deep learning models can be implemented and optimised to categorise retinal diseases from fundus images. The best model among the first attempts was MobileNetV2, with an accuracy of 89.81%. This surpassed VGG16, InceptionV3, and a custom CNN model. Additionally, the Snake Optimiser was utilised to explore hyperparameters (such as dense layer units, dropout rates, learning rates, and batch sizes) to improve performance.

This optimisation helped a lot, enabling the model to reach test accuracy of 96.33%. The optimised MobileNetV2 model generalised well to all classes; most notably, cataracts achieved 100%, 98%, and 99% accuracy, recall, and F1-score, respectively. Similar high metrics were achieved for diabetic retinopathy, while good results were obtained with glaucoma and normal cases as well.

Snake Optimiser was an ideal optimiser that was deployed, and the contribution was highly notable. Since this was an experimental process, such an optimiser will definitely play a role in current deep learning models for medical image analysis. The obtained results have shown that combining deep learning with bio-inspired optimisation algorithms can lead to dependable diagnostic systems that maximise performance while minimising complexity. An additional benefit of the proposed method is that it improves ophthalmologists' efficiency while enabling timely diagnosis of retinal diseases. This, in turn, helps in mitigating vision loss.

ISSN: 2408-7920

Future research in this domain could explore integrating multimodal data with real-time applications to further extend the utility of such systems in clinical practice.

REFERENCES

Abdel-Hamid, L. (2022). TWEEC: Computer-aided glaucoma diagnosis from retinal images using deep learning techniques. *International Journal of Imaging Systems and Technology*, *32*(1), 387–401. https://doi.org/https://doi.org/10.1002/ima.22621

Ayzenberg, V., Kamps, F. S., Dilks, D. D., & Lourenco, S. F. (2022). Skeletal representations of shape in the human visual cortex. *Neuropsychologia*, *164*, 108092. https://doi.org/https://doi.org/10.1016/j.neuropsychologia.2021.108092

Bourne, R. R. A., Stevens, G. A., White, R. A., Smith, J. L., Flaxman, S. R., Price, H., Jonas, J. B., Keeffe, J., Leasher, J., & Naidoo, K. (2013). Causes of vision loss worldwide, 1990–2010: a systematic analysis. *The Lancet Global Health*, *1*(6), e339–e349.

Chang, J., Lee, J., Ha, A., Han, Y. S., Bak, E., Choi, S., Yun, J. M., Kang, U., Shin, I. H., & Shin, J. Y. (2021). Explaining the rationale of deep learning glaucoma decisions with adversarial examples. *Ophthalmology*, *128*(1), 78–88.

Congdon, N., O'Colmain, B., Klaver, C. C., Klein, R., Muñoz, B., Friedman, D. S., Kempen, J., Taylor, H. R., & Mitchell, P. (2004). Causes and prevalence of visual impairment among adults in the United States. *Archives of Ophthalmology (Chicago, Ill.: 1960)*, *122*(4), 477–485.

Elloumi, Y. (2021). Mobile aided system of deep-learning based cataract grading from fundus images. *International Conference on Artificial Intelligence in Medicine*, 355–360.

Farooq, M. S., Arooj, A., Alroobaea, R., Baqasah, A. M., Jabarulla, M. Y., Singh, D., & Sardar, R. (2022). Untangling computer-aided diagnostic system for screening diabetic retinopathy based on deep learning techniques. *Sensors*, *22*(5), 1803.

Gour, N., & Khanna, P. (2021). Multi-class multi-label ophthalmological disease detection using transfer learning based convolutional neural network. *Biomedical Signal Processing and Control*, *66*, 102329. https://doi.org/https://doi.org/10.1016/j.bspc.2020.102329

Hu, K., Zhang, Z., Niu, X., Zhang, Y., Cao, C., Xiao, F., & Gao, X. (2018). Retinal vessel segmentation of color fundus images using multiscale convolutional neural network with an improved cross-entropy loss function. *Neurocomputing*, *309*. https://doi.org/10.1016/j.neucom.2018.05.011

Jiang, J., Lei, S., Zhu, M., Li, R., Yue, J., Chen, J., Li, Z., Gong, J., Lin, D., & Wu, X. (2021). Improving the generalizability of infantile cataracts detection via deep learning-based lens partition strategy and multicenter datasets. *Frontiers in Medicine*, *8*, 664023.

African Journal of Applied Research
Vol. 12, No. 4 (2026), pp.350-376
http://www.ajaronline.com
https://doi.org/10.26437
Received November22, 2025
Peer reviewed: April 15, 2026
Revised: May 15, 2026
Published: June 30, 2026

Junayed, M. S., Islam, M. B., Sadeghzadeh, A., & Rahman, S. (2021). CataractNet: An automated cataract detection system using deep learning for fundus images. *IEEE Access*, *9*, 128799–128808.

Junjun, H., Li, C., Ye, J., Qiao, Y., & Gu, L. (2021). Multi-label ocular disease classification with a dense correlation deep neural network. *Biomedical Signal Processing and Control*, *63*, 102167. https://doi.org/10.1016/j.bspc.2020.102167

Keenan, T. D. L., Chen, Q., Agrón, E., Tham, Y.-C., Goh, J. H. L., Lei, X., Ng, Y. P., Liu, Y., Xu, X., Cheng, C.-Y., Bikbov, M. M., Jonas, J. B., Bhandari, S., Broadhead, G. K., Colyer, M. H., Corsini, J., Cousineau-Krieger, C., Gensheimer, W., Grasic, D., … Group, =AREDS Deep Learning Research. (2022). DeepLensNet: Deep Learning Automated Diagnosis and Quantitative Classification of Cataract Type and Severity. *Ophthalmology*, *129*(5), 571–584. https://doi.org/10.1016/j.ophtha.2021.12.017

Kumar, K. S., & Singh, N. P. (2023). Retinal disease prediction through blood vessel segmentation and classification using ensemble-based deep learning approaches. *Neural Computing and Applications*, *35*(17), 12495–12511.

Li, J. Q., Welchowski, T., Schmid, M., Letow, J., Wolpers, C., Pascual-Camps, I., Holz, F. G., & Finger, R. P. (2020). Prevalence, incidence and future projection of diabetic eye disease in Europe: a systematic review and meta-analysis. *European Journal of Epidemiology*, *35*(1), 11–23. https://doi.org/10.1007/s10654-019-00560-z

Li, T., Bo, W., Hu, C., Kang, H., Liu, H., Wang, K., & Fu, H. (2021). Applications of deep learning in fundus images: A review. *Medical Image Analysis*, *69*, 101971. https://doi.org/https://doi.org/10.1016/j.media.2021.101971

Luo, X., Li, J., Chen, M., Yang, X., & Li, X. (2021). Ophthalmic disease detection via deep learning with a novel mixture loss function. *IEEE Journal of Biomedical and Health Informatics*, *25*(9), 3332–3339.

Mahmoud, M. H., Alamery, S., Fouad, H., Altinawi, A., & Youssef, A. E. (2023). RETRACTED ARTICLE: An automatic detection system of diabetic retinopathy using a hybrid inductive machine learning algorithm. *Personal and Ubiquitous Computing*, *27*(3), 751–765.

Mushtaq, G., & Siddiqui, F. (2021). Detection of diabetic retinopathy using deep learning methodology. *IOP Conference Series: Materials Science and Engineering*, *1070*(1), 012049.

Nawaz, M., Nazir, T., Javed, A., Tariq, U., Yong, H.-S., Khan, M. A., & Cha, J. (2022). An efficient deep learning approach to automatic glaucoma detection using optic disc and optic cup localization. *Sensors*, *22*(2), 434.

ISSN: 2408-7920

African Journal of Applied Research
Vol. 12, No. 4 (2026), pp.350-376
http://www.ajaronline.com
https://doi.org/10.26437
Received November22, 2025
Peer reviewed: April 15, 2026
Revised: May 15, 2026
Published: June 30, 2026

Orfao, J., & van der Haar, D. (2021). *A Comparison of Computer Vision Methods for the Combined Detection of Glaucoma, Diabetic Retinopathy and Cataracts* (pp. 30–42). https://doi.org/10.1007/978-3-030-80432-9_3

Pahuja, R., Sisodia, U., Tiwari, A., Sharma, S., & Nagrath, P. (2022). A Dynamic approach of eye disease classification using deep learning and machine learning model. In *Proceedings of Data Analytics and Management: ICDAM 2021, Volume 1* (pp. 719–736). Springer.

Playout, C., Duval, R., & Cheriet, F. (2019). A Novel Weakly Supervised Multitask Architecture for Retinal Lesions Segmentation on Fundus Images. *IEEE Transactions on Medical Imaging*, *38*, 2434–2444. https://api.semanticscholar.org/CorpusID:85515615

Prananda, A. R., Frannita, E. L., Hutami, A. H. T., Maarif, M. R., Fitriyani, N. L., & Syafrudin, M. (2022). Retinal nerve fiber layer analysis using deep learning to improve glaucoma detection in eye disease assessment. *Applied Sciences*, *13*(1), 37.

Ryu, G., Lee, K., Park, D., Park, S. H., & Sagong, M. (2021). A deep learning model for identifying diabetic retinopathy using optical coherence tomography angiography. *Scientific Reports*, *11*(1), 23024.

Tham, Y.-C., Goh, J. H. L., Anees, A., Lei, X., Rim, T. H., Chee, M.-L., Wang, Y. X., Jonas, J. B., Thakur, S., & Teo, Z. L. (2022). Detecting visually significant cataract using retinal photograph-based deep learning. *Nature Aging*, *2*(3), 264–271.

Thanki, R. (2022). Deep Learning Based Model for Fundus Retinal Image Classification. *International Conference on Soft Computing and Its Engineering Applications*, 238–249.

Thanki, R. (2023). A deep neural network and machine learning approach for retinal fundus image classification. *Healthcare Analytics*, *3*, 100140.

Veena, H. N., Muruganandham, A., & Kumaran, T. S. (2022). A novel optic disc and optic cup segmentation technique to diagnose glaucoma using deep learning convolutional neural network over retinal fundus images. *Journal of King Saud University-Computer and Information Sciences*, *34*(8), 6187–6198.

ISSN: 2408-7920